AGU PUBLICATIONS

Geophysical Research Letters

RESEARCH LETTER
10.1002/2016GL071178

Key Points:
- Notable regional differences exist in the SST and chl a response to storms
- Surface bloom responses are associated with different chl a sources in the upper ocean
- DINEOF is a robust method for analyzing daily storm induced SST and chl a responses

Supporting Information:
- Supporting Information S1
- Figure S1
- Figure S2
- Table S1

Correspondence to:
R. He,
rhe@ncsu.edu

Citation:
Shropshire, T., Y. Li, and R. He (2016), Storm impact on sea surface temperature and chlorophyll *a* in the Gulf of Mexico and Sargasso Sea based on daily cloud-free satellite data reconstructions, *Geophys. Res. Lett.*, *43*, 12,199–12,207, doi:10.1002/2016GL071178.

Received 11 SEP 2016
Accepted 14 NOV 2016
Accepted article online 16 NOV 2016
Published online 14 DEC 2016

Storm impact on sea surface temperature and chlorophyll *a* in the Gulf of Mexico and Sargasso Sea based on daily cloud-free satellite data reconstructions

Taylor Shropshire[1], Yizhen Li[2], and Ruoying He[3]

[1]Department of Earth, Ocean and Atmospheric Sciences, Center for Ocean-Atmospheric Prediction Studies, Florida State University, Tallahassee, Florida, USA, [2]Department of Applied Ocean Physics and Engineering, Woods Hole Oceanographic Institution, Woods Hole, Massachusetts, USA, [3]Department of Marine, Earth and Atmospheric Sciences, North Carolina State University, Raleigh, North Carolina, USA

Abstract Upper ocean responses to tropical storms/hurricanes have been extensively studied using satellite observations. However, resolving concurrent sea surface temperature (SST) and chlorophyll *a* (chl *a*) responses along storm tracks remains a major challenge due to extensive cloud coverage in satellite images. Here we produce daily cloud-free SST and chl *a* reconstructions based on the Data INterpolating Empirical Orthogonal Function method over a 10 year period (2003–2012) for the Gulf of Mexico and Sargasso Sea regions. Daily reconstructions allow us to characterize and contrast previously obscured subweekly SST and chl *a* responses to storms in the two main storm-impacted regions of the Atlantic Ocean. Statistical analyses of daily SST and chl *a* responses revealed regional differences in the response time as well as the response sensitivity to maximum sustained wind speed and translation speed. This study demonstrates that SST and chl *a* responses clearly depend on regional ocean conditions and are not as universal as might have been previously suggested.

1. Introduction

Tropical storms (wind speeds $> 17.5\ m\ s^{-1}$) and hurricanes (wind speeds $> 33\ m\ s^{-1}$) have been shown to significantly affect the ocean's surface physical and biological properties. Factors influential to ocean physical and biological responses to storm events include storm intensity (wind speed), translation speed, and size (radius of gale force wind), as well as local hydrodynamics and water column distribution of nutrients and phytoplankton biomass [*Babin et al.,* 2004]. The physical response of the upper ocean to storms mainly consists of a decrease in sea surface temperature (SST) associated with an uplifted thermocline, deepening of the mixed layer, transient upwelling induced by Ekman pumping, and a near-inertial response [*Jacob et al.,* 2000; *Price,* 1981; *Sanford et al.,* 1987; *Shay and Elsberry*, 1987]. The corresponding biological response has been observed by satellite, to a degree, during and immediately after storm events [e.g., *Babin et al.,* 2004; *Davis and Yan*, 2004; *Gierach and Subrahmanyam,* 2008; *Hanshaw et al.,* 2008; *Lin et al.,* 2003; *Merritt-Takeuchi and Chiao,* 2013; *Walker et al.,* 2005], and elevated surface pigments are a consequence of entrainment of subsurface chl *a*-rich water and/or new production due to the injection of nutrients from below the nutricline [*Gierach and Subrahmanyam,* 2008; *Walker et al.,* 2005].

Physical characteristics of tropical storms/hurricanes vary on short time scales (hours to days) as storms evolve. In addition, a storm swath typically passes through different regional oceans associated with a variety of vertical thermal structures and phytoplankton-nutrient distributions. Therefore, a regionally dependent SST and chl *a* response occurring on subweekly time scales would be an expected consequence of storm forcing on the ocean. Past studies have attempted to analyze the upper ocean SST and chl *a* response to tropical cyclones by taking advantage of rather rare, low cloud cover opportunities [e.g., *Walker et al.,* 2005], using composite satellite images [e.g., *Babin et al.,* 2004; *Merritt-Takeuchi and Chiao,* 2013], or microwave radiometers to measure SST alone [e.g., *Lin et al.,* 2003; *Wentz et al.,* 2000]. Although 7 day SST and 8 day composite chl *a* images have been shown to resolve the temporal variability of the SST and chl *a* response on weekly or longer time scales, these studies cannot resolve the daily to subweekly response variability. Furthermore, the SST and chl *a* responses have likely much evolved by the time the first cloud-free composite images are available, and therefore, estimates and interpretations of ocean SST and chl *a* responses based on these images may be biased.

In this study, we seek to overcome the common cloud cover problem in satellite observations and to better represent along-track SST and chl *a* responses to tropical storms/hurricanes (herein referred to as storms). We apply the Data INterpolating Empirical Orthogonal Function (DINEOF) method [*Alvera-Azcárate et al.,* 2005] to reconstruct 10 year (2003–2012) daily cloud-free SST and chl *a* images, from which a statistical assessment of the concurrent SST and chl *a* response to storms was performed. Our specific goals were to (1) determine and compare the timing of the regional SST and chl *a* response by analyzing variations in response magnitude before, during, and after storm passage and (2) investigate the sensitivity of these regional responses to two important characteristics of storms: maximum sustained wind speed (herein referred to as wind speed) and translation speed. In doing so, we aim to identify characteristic regional similarities and differences in previously obscured subweekly SST and chl *a* responses in the two main storm impacted regions of the Atlantic Ocean: the Yucatan Channel-Gulf of Mexico (GoM) region and the Mid-Atlantic Bight-Sargasso Sea (SS) region.

2. Data and Methods

2.1. Satellite SST and Chl *a*

In this study, we constructed daily cloud-free SST and chl *a* data for the GoM and SS based on daily daytime Moderate Resolution Imaging Spectroradiometer (MODIS) SST and chl *a* data from January 2003 to December 2012 using the Data INterpolating Empirical Orthogonal Function (DINEOF) method. These two regional oceans are the foci of many earlier studies investigating ocean response to tropical cyclones [e.g., *Babin et al.,* 2004; *Foltz et al.,* 2015; *Gierach and Subrahmanyam,* 2008; *Hanshaw et al.,* 2008; *Walker et al.,* 2005] but have yet to be compared. The DINEOF method identifies dominant spatial and temporal patterns and fills in missing points accordingly. For details of this method, we refer readers to earlier publications [*Alvera-Azcárate et al.,* 2005; *Alvera-Azcárate et al.,* 2007; *Li and He*, 2014; *Miles and He*, 2009, 2010*; Zhao and He,* 2012]. The relative advantage of this approach is that it applies a random cross validation to further validate the reconstruction (i.e., assuming a portion of the existing data is cloud covered and validating the reconstruction against the existing data). Previous analyses have clearly shown that DINEOF is able to reasonably capture the missing data given that the cloud cover is less than 95% [e.g., *Alvera-Azcárate et al.,* 2005], which is the maximum cloud cover used for reconstructions in this study. In our own analysis (not shown) we find that below 95% cloud cover daily variations in SS cloud cover have little influence (all statistically significant correlations >0.75) on the ability of the reconstruction to capture the SST variability in buoy observations.

Similar to *Alvera-Azcárate et al.* [2007], *Miles et al.* [2009], and *Li and He* [2014], we utilized a multivariate adaptation of DINEOF for the reconstruction in this study. The concurrent SST and chl *a*, and 1 day lagged SST were used to reconstruct SST fields, whereas concurrent SST and chl *a*, and 1 day lagged chl *a* were used to reconstruct chl *a* fields. A natural logarithmic scale transformation was applied to the chl *a* field before the reconstruction, following the same approach used in *Li and He* [2014]. We chose 1 day as the lag time because we found it produced the best reconstruction results. The resulting 10 year reconstructed SST and chl *a* for the NW Atlantic Ocean were used for further analyses.

2.2. Storm Characteristics

We tracked the life history of each tropical storm/hurricane that occurred over the 10 year study period in the Atlantic Ocean using the 6-hourly storm center position and intensity data from the National Hurricane Center archive (http://www.nhc.noaa.gov/data/). For each storm, the average daily position (i.e., latitude and longitude of the storm center), wind speeds, and translation speeds (calculated by taking the difference in distance between adjacent track points) were obtained. If the impact zone of a given daily track point was located inside either the GoM or SS domain and at least one track point on the storm track was located inside the domain—defining the storm as a GoM or SS storm—we recorded the corresponding date. DINEOF SST and chl *a* images at these times were subsequently extracted for further analysis. Overall, 292 (339) track points and their associated daily SST and chl *a* images were identified for the GoM (SS). Among these, 156 (53%) track points for the GoM and 215 (63%) track points for the SS were associated with gale force winds ($>$17.5 m/s). These subsets were used to perform statistical analyses on the regional ocean response time as well as the response sensitivity to wind and translation speed.

2.3. Impact Zone

Following an approach similar to that of *Babin et al.* [2004], we defined for each storm the prestorm conditions by averaging the SST and chl *a* images from a period of 3 weeks to 1 week before the date associated with the first track point that is within the domain. All track points on a given storm track were included in the analysis if at least one track point entered the domain. We examined the concurrent daily ocean SST and chl *a* response using a 200 km radius impact zone to measure storm-induced changes in SST and surface chl *a*. That is, ΔSST and Δchl *a* were calculated for each daily track point by taking the difference in the spatial mean of SST and chl *a* within the track points' impact zone between the prestorm condition image and the image associated with the track point.

The use of a 200 km radius impact zone for sampling surface ocean response to storms is comparable to previous studies [e.g., *Babin et al.,* 2004; *Hanshaw et al.,* 2008] and aligns with average storm size parameters in the North Atlantic [*Kimball and Mulekar*, 2004]. When comparing results derived using the same rectangular impact cell (36,300 km^2) adopted by *Babin et al.* [2004] versus using a circular impact zone (126,500 km^2) adopted in this study, we found that there was insignificant difference between the average ΔSST responses calculated (-0.74°C versus -0.69°C) and the average Δchl *a* responses calculated (16.4% versus 14.9%). We also note that changes in impact zone radius did influence the response magnitude but did not influence the response timing or sensitivity—on which our conclusions are based.

2.4. Response Analysis

To temporally characterize the regional response, we calculated the timing of the maximum response in |SST| and chl *a*. The response for each individual track point was calculated using the same impact zone approach as described above, only now we allowed the reconstructed image to vary by $\pm$7 days. The response was calculated for each day, and the day associated with the largest decrease in SST and largest increase in chl *a* was recorded.

To examine the response sensitivity to storm forcing, we compared the regional ocean responses to wind speed and translation speeds with zero time lag (i.e. storm day images) based on our findings of short average maximum response times (0.55–1.39 days, see section 3.2) of SST and chl *a* and also because we were interested in examining concurrent ocean responses to storm forcing. Additionally, for a cleaner illustration of a spectrum of wind regimes (i.e., weak tropical storms to hurricanes), track points were binned into intervals of 3 m/s for wind speed (from 17.5 to 47.5 m/s) and 1 m/s for translation speed (from 0 to 10 m/s). For data quality control, we excluded track points where either ΔSST or Δchl *a* was greater than two standard deviations from the mean. The resulting binned data went through the same quality control and were then used to compute linear regressions between both ΔSST and Δchl *a* against wind speed and translation speed.

3. Results

3.1. Validation of DINEOF Reconstruction

Because there are no long-term in situ chl *a* data available, our validation of the DINEOF method focused on cloud-free SST reconstruction, utilizing in situ temperature data from the National Data Buoy Center (http://www.ndbc.noaa.gov/). We selected five buoys in the GoM and seven in the SS (locations in Figure 1) that had limited data gaps and were collectively representative of the regional ocean. Daily averaged SST from buoys were compared to DINEOF SST reconstruction by linearly interpolating the closest point on reconstructed images to buoy locations, and these comparisons were only conducted during storm dates.

It is worth noting that while no long-term chl *a* data are available preventing a similar analysis, the magnitude of chl *a* anomalies and the chl *a* regression against wind speed computed from reconstructions in this study are comparable to previous studies. A change of 20 m s^{-1} in wind speed was estimated to resulted in a 20% increase in chl *a* by *Babin et al.* [2004] and 19% by *Hanshaw et al.* [2008], which is similar to our finding of 16%. In addition, the characteristic regional chl *a* responses identified here align with what we would expect to find based on regional subsurface nutrient data as well as storm entrainment estimates (see section 4). To our knowledge the DINEOF method has not been used to estimate the highly dynamic ocean response to tropical cyclones; however, the method has been shown to be successful in capturing phytoplankton blooms—a highly dynamic process—in the Gulf of Maine [e.g., *Li and He,* 2014].

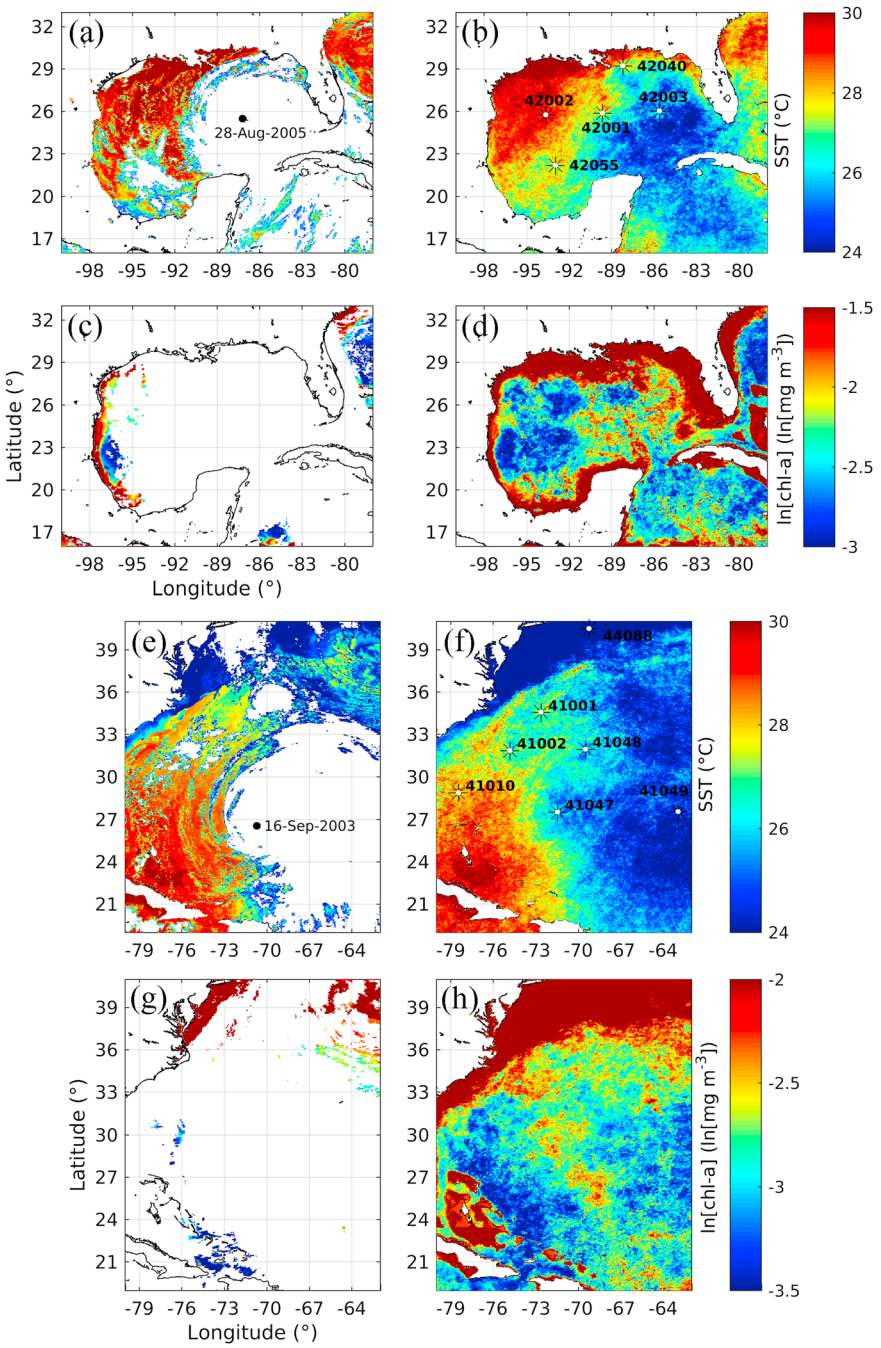

Figure 1. Raw MODIS 4 km satellite data and their corresponding DINEOF reconstruction during (a–d) Hurricane Katrina in GoM and (e–h) Hurricane Isabel in the SS. GoM domain overlaid with MODIS SST image during Hurricane Katrina on 28 August 2005 (Figure 1a). SST reconstruction (Figure 1b) of the same day as Figure 1a, with buoy locations indicated. GoM domain overlaid with MODIS chl *a* image (Figure 1c) during the same day as Figure 1a. Chl *a* reconstruction (Figure 1d) of the same day as Figure 1a. SS domain overlaid with MODIS SST image during Hurricane Isabel on 16 September 2003 (Figure 1e). SST reconstruction (Figure 1f) of the same day as in Figure 1e, with buoy locations indicated. SS domain overlaid with MODIS chl *a* image (Figure 1g) during the same day as Figure 1e. Chl *a* reconstruction (Figure 1h) of the same day as Figure 1e.

The utility of using the DINEOF method to analyze SST and chl *a* responses from daily cloud-free reconstructions is demonstrated in both regions by significant correlations with buoy observations during storm days (Table S1 in the supporting information). Average correlation for the GoM (SS) was 0.75 (0.87). The mean bias and RMS values for the GoM (SS) were 1.65°C (1.41°C) cooler and 1.90 (1.83), respectively. Some potential

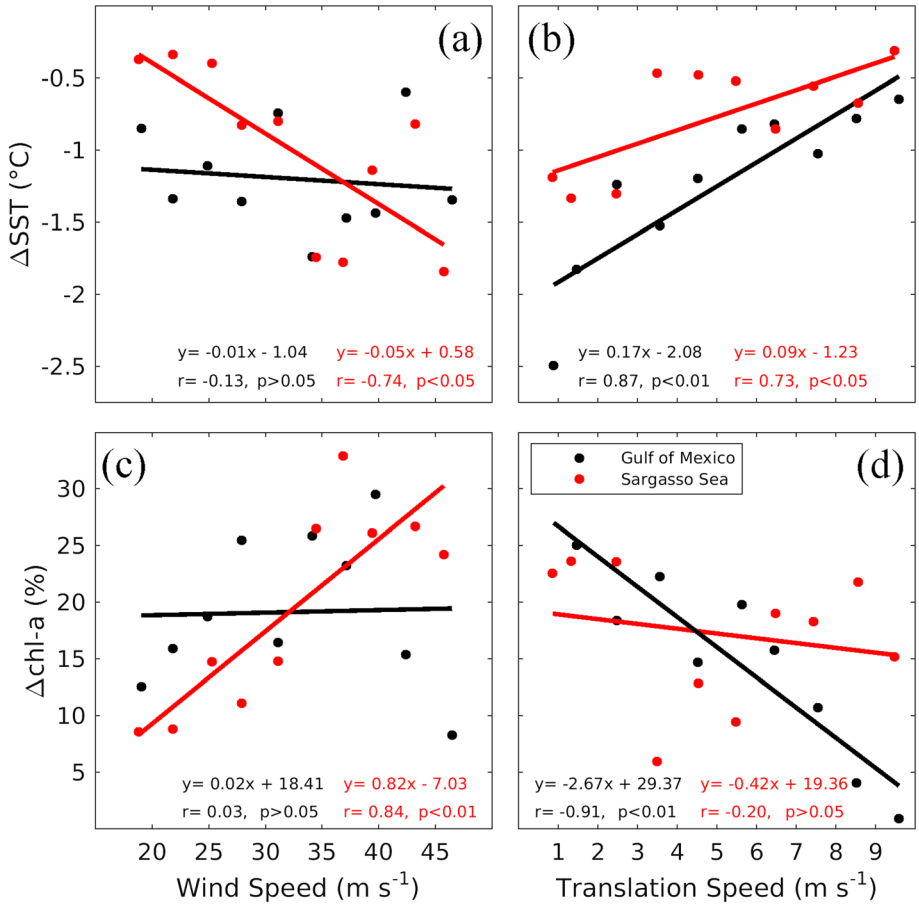

Figure 2. Relationship between regional (a and b) ΔSST and (c and d) Δchl *a* in response and daily averaged maximum sustained (a and c) wind speed and storm (b and d) translation speed for the GoM and SS. Each data point represents the mean responses within a bin.

errors that could have contributed to the difference between buoy-measured SST and DINEOF include spatial offsets between buoy locations and the DINEOF SST 4 km footprint as well as differences between satellite-derived ocean skin temperature and buoy bulk temperature measured 1 to 2 m below the surface. In spite of these potential errors, the statistically significant correlations between reconstruction and in situ data during storm events suggest that DINEOF is a robust method for analysing daily SST and chl *a* response time and sensitivity to storm forcing as it captures the major response *variability*—on which our analysis is based—associated with storm events (animation of model-data comparison during Hurricane Katrina is available at http://oceanus.meas.ncsu.edu/Katrina/).

3.2. Ocean Responses to Storms

When examining the regional SST and chl *a* response before, during, and after storm passage (i.e. $\pm$7 days), we found that on average, the timing of the maximum SST and chl *a* response (herein referred to as response time) is more tightly coupled in the GoM in comparison to the SS. The GoM and SS response time of SST was found to occur 0.99 ± 2.95 day and 0.55 ± 3.94 day after storm passage, respectively (Figure S1a). The chl *a* response took longer to occur, with a response time of 1.06 ± 3.44 days in the GoM and 1.39 ± 4.22 days in the SS (Figure S1b). The statistical significance of the SST and chl *a* response time between study regions was investigated using an unpaired *t* test. We found the differences in regional SST (chl *a*) response time to be statistically significant within a 95% (90%) confidence interval.

The sensitivity of ocean SST and chl *a* response to storm forcing (i.e., wind speed and translation speed) presents another interesting regional difference between the GoM and SS. Previously, surface cooling (i.e., $-\Delta$SST) and increasing surface chl *a* (i.e., $+\Delta$chl *a*) have been presumed to be proportional to wind speed

Table 1. Relationships (Linear Regression Coefficients) of Both ΔSST and ΔChl *a* With Daily Averaged Maximum Sustained Wind Speed and Translation Speed[a]

	ΔSST		ΔChl *a*	
	GoM	SS	GoM	SS
Wind speed	−0.01 (−0.13)	−0.05 (−**0.74**)	0.02 (0.03)	0.82 (**0.84**)
Translation speed	0.17 (**0.87**)	0.09 (**0.73**)	−2.67 (−**0.91**)	−0.42 (−0.20)
Response time	0.99	0.55	1.06	1.39

[a]Correlation values for response to storm forcing are given in parentheses, where bold numbers indicate statistical significance. The response time metric for each region is given in the last row.

and inversely proportional to translation speed [*Cione and Uhlhorn,* 2003; *Babin et al.,* 2004]. However, in our analysis we found that the SST and chl *a* response in the GoM (SS) exhibits a strong dependence on translation (wind) speed and little to no dependence on wind (translation) speed (Figure 2).

Linear regression analyses revealed that SST and chl *a* responses in the GoM are both more sensitive (i.e., regression coefficients of greater magnitude) to translation speed than in the SS, and more correlated with translation speed than with wind speed. In contrast, responses in the SS are both more sensitive to wind speed than in the GoM, and more correlated with wind speed compared to translation speed. Table 1 summarizes the regional contrast. The statistical significance between regressions was investigated using a regression *z* test [*Paternoster et al.,* 1998]. All differences in linear regression coefficients between regions are statistically significant within a 95% confidence interval except that of SST as a function of translation speed (Figure 2c), which is significant within a 90% confidence interval.

In terms of frequency, we found that the typical biological (+Δchl *a*) and physical (−ΔSST) responses occurred more often in the GoM than in the SS. Relative to their prestorm conditions, of the 156 (215) track points in the GoM (SS), 84% (75%) were associated with an increase in surface chl *a*. Concurrently, a decrease in SST was observed at 92% (70%) of GoM (SS) track points. Although the lack of chl *a* observations and error associated with SST reconstructions prevents the use of statistical analyses to directly compare the magnitude of the SST and chl *a* response between regions, it is worth noting that after the removal of outliers the maximum chl *a* increase (the greatest SST drop) in the GoM was 70% (3.48°C) similar to 68% (3.33°C) in the SS. The average response ($\pm$1 standard deviation) for the GoM (SS) was found to be $18 \pm 19\%$ ($15 \pm 21\%$) and 1.17 ± 0.89°C (0.69 ± 1.14°C), respectively.

4. Discussion and Conclusions

Many case studies have been conducted associated with the topic of SST and chl *a* responses induced by storms. One study in particular by *Gierach and Subrahmanyam* [2008] complements the present study nicely. In their study, they investigated three category 5 hurricanes in the GoM (Katrina, Rita, and Wilma) and concluded that the source of chl *a* contributing to the response was different between storms. Based on the estimated storm entrainment depths, regional nutricline depth, and deep chlorophyll maximum (DCM) depth they argued that the observed chl *a* anomaly during hurricane Katrina and Rita was a result of both new production driven by nutrient influx to the surface and chl *a* entrainment from the subsurface maximum, while the response from Hurricane Wilma was associated with only the latter. Although this case study and others like it are useful in initially shaping our understanding of the SST and chl *a* response to storms, a statistical approach is greatly needed to provide a comprehensive depiction of the biophysical interactions during storms in both regions. Such an approach will avoid possible biased generalizations based on only a few storms and thus further our understanding past isolated events. Meeting this need is the primary focus of this paper.

While SST signatures associated with storms are relatively well understood, previous studies have been left to speculate on the source of chl *a* leading to positive surface chl *a* anomalies observed after storm passages using composite images. By measuring daily SST and chl *a* response of storm track points instead of evaluating individual storms on weekly time scales as traditionally done, our approach allows us to capture the chl *a* response evolution on time scales more appropriate for analyzing phytoplankton responses in the ocean.

In order for storms to induce a chl *a* response detectable by satellites, either a strong DCM must be present and shallow enough to be entrained by storm-induced mixing, and/or the regional nutricline must be shallow

enough that injection of nutrients is possible which subsequently supports new production in the surface ocean. The latter is an intrinsic biological response, whereas the former is a physical displacement of biomass. Indeed, distinguishing between these two chl *a* sources is crucial if we seek to understand the impact storms have on surface ocean biology and chemistry. In addition, there is reason to believe that the biogeochemical impact of these storm-induced chl *a* responses may be substantial considering that the integrated impact of hurricanes has shown to have a significant contribution (22%) in the interannual chl *a* variability over hurricane season [*Foltz et al.,* 2015].

Based on our SST and chl *a* response time analysis, we find the SST and chl *a* response time to be more synchronous in the GoM (Table 1). The tightly coupled SST and chl *a* response time found in the GoM suggests the positive surface chl *a* anomaly observed after storm passage is dominated by entrainment. In contrast, the less coupled SST and chl *a* response time, associated with a slower more variable chl *a* response time, found in the SS suggests nutrient injection is likely more significant compared to the GoM. However, entrainment of chl *a*-rich water is likely the dominant signal in both systems based on the rapid increase of chl *a* during and within a day after storm passage. It is worth noting the chl *a* response time in the GoM (1.06 ± 3.44 days) identified here is faster than the 3–4 days response time previously identified by *Walker et al.* [2005].

In addition to regional differences in the SST and chl *a* response time, our results show clear differences in regional SST and chl *a* response to storms as a function of wind and translation speed. Based on the coefficient of determination (r^2) associated with the regression in Figure 2d, translation speed explains only 4% of the variance of the chl *a* response in the SS, which is similar to *Babin et al.*'s [2004] finding of 6% after analyzing 13 hurricanes in an area comparable to our SS domain. In contrast, we find that translation speed of a storm explains 83% of the chl *a* response in the GoM. In terms of wind speed, we find that in the SS it explains 71% of the variance in the chl *a* response, comparable to *Babin et al.*'s [2004] finding of 58%. Yet based on our analysis, wind speed only explains 0.1% of the variance in GoM chl *a* response. Relationships between regional SST response and storm forcing exhibit comparable r^2 values in both regions.

Mechanistically speaking, a regional SST and chl *a* response would be sensitive to wind speed, as seen in the SS, if the mixed layer and the nutricline are shallow such that almost any entrainment results in a measurable response. In contrast, a regional SST and chl *a* response that is sensitive to translation speed, as seen in the GoM, would imply the existence of a deeper mixed layer resulting in a response that depends on slow translating storms to allow for upwelling of deeper cold, chl *a*/nutrient-rich water via Ekman pumping.

Utilizing the National Ocean Data Center (https://www.nodc.noaa.gov/), World Ocean Atlas 2013 V2 Climatological Nitrate 1° Statistical Mean product, we investigated the vertical distribution of nutrients during hurricane season in the GoM and SS by spatially averaging nitrate ($[NO_3^-]$) profiles across depths from 0 to 200 m during 1 June to 1 November, totaling 420 (836) profiles for the GoM (SS) (Figure S2). Although a nitracline was difficult to distinguish in both regions across hurricane season, we indeed found that relative to the surface, $[NO_3^-]$ increases at a deeper point (~35 m) in the GoM and at a shallower point (~5 m) in the SS (herein referred to as the nurtricline). Similarly, a regional thermocline averaged over hurricane season was difficult to distinguish; however, in the open ocean where light penetrates deep into the water column nutriclines are often closely paired with the thermocline.

Given the regional nutricline depths storms entraining water from 0 to 35 m would induce a greater increase in surface $[NO_3^-]$ and subsequently stimulate more new production in the SS compared to the GoM, respective of the region. In contrast, the deeper nutricline in the GoM would limit the potential of storms to entrain nutrient-rich water to the surface. However, the deeper nutricline and larger gradient of $[NO_3^-]$ at depth would likely result in a stronger DCM and thus allow for a greater contribution of chl *a*-rich water in this region. This would explain the more coupled SST and chl *a* response associated with a slower SST response and a faster chl *a* response found in the GoM as well as the less coupled SST and chl *a* response associated with a faster SST response and slower chl *a* response found in the SS (Table 1).

To investigate the frequency of storms that would result in such an outcome and thereby assess the validity of our interpretation, we estimate the entrainment depth of storms in both regions using the analytical solution $\eta = \tau(\rho f \mu)$ [*Price,* 1981]; where η is the displacement, τ is wind stress, ρ is density, f is the Coriolis parameter, and μ is translation speed of the storm. Across all daily storm track points, isopycnal displacement ranged

from 1.16 to 53.83 m and 0.44 to 61.44 m for the GoM and SS, respectively. Within this range, we indeed find that a strong majority (95% for the GoM and 96% for the SS) of track points were associated with wind and translation speeds that resulted in the displacement of isopycnals to depths shallower than 35 m.

In agreement with climatological [NO_3^-] data and storm entrainment depth estimates, the results from this study reveal clear regional differences in previously obscured subweekly SST and chl *a* response to storms. Based on our response time analysis, we found that the relative contribution of chl *a*-rich water entrainment, and new production can be notably region dependent. Additionally, the differences in regional SST and chl *a* response sensitivity suggests that ocean response to storms is not as universal as might have been previously implied. An important caveat, however, is that the data set includes more mild than strong storms, resulting in fewer data points in high wind speed bins. So although we found that the chl *a* response in the GoM does not show a significant response to wind speed over the entire storm wind spectrum, it is possible that at lower wind speeds a stronger relationship exists. It is also worth noting that while regressions provide a useful statistical relationship for contrasting the sensitivity of the regional ocean response to storms, the functions presented here are associated with large bars of variance and therefore should not be used for predictive purposes.

In summary, we constructed 10 year daily regional cloud-free SST and chl *a* databases for the Gulf of Mexico and Sargasso Sea. The data set was used to identify and characterize differences in previously obscured subweekly regional SST and chl *a* ocean response. In doing so, we (1) demonstrated the utility of the DINEOF method in studying daily variability in SST and chl *a* ocean responses to storms; (2) distinguished characteristic regional chl *a* response times associated with different sources of chl *a*; and (3) revealed sensitivity differences in regional SST and chl *a* response as a function of wind speed and translation speed. Detailed quantification of such differences in regional ocean response identified in this study, namely, the relative contribution of chl *a* sources in the storm-induced chl *a* anomalies, requires more subsurface observations in conjunction with the aid of coupled biophysical modeling.

Acknowledgments

Research support provided by Gulf of Mexico Research Initiative/GISR through grant 02-S130202, NOAA grant NA11NOS0120033, and NASA grants NNX12AP84G and NNX13AD80G are much appreciated. We thank J. Warrillow for her editorial assistance. For cloud-free SST and chl *a* product presented in the work, please contact the corresponding author at rhe@ncsu.edu.

References

Alvera-Azcárate, A., A. Barth, M. Rixen, and J. M. Beckers (2005), Reconstruction of incomplete oceanographic data sets using empirical orthogonal functions: Application to the Adriatic Sea surface temperature, *Ocean Model.*, *9*(4), 325–346, doi:10.1016/j.ocemod.2004.08.001.

Alvera-Azcárate, A., A. Barth, J. M. Beckers, and R. H. Weisberg (2007), Multivariate reconstruction of missing data in sea surface temperature, chlorophyll, and wind satellite fields, *J. Geophys. Res.*, *112*, C03008, doi:10.1029/2006JC003660.

Babin, S. M., J. A. Carton, T. D. Dickey, and J. D. Wiggert (2004), Satellite evidence of hurricane-induced phytoplankton blooms in an oceanic desert, *J. Geophys. Res.*, *109*, C03043, doi:10.1029/2003JC001938.

Cione, J. J., and W. E. Uhlhorn (2003), Sea surface temperature variability in hurricanes: Implications with respect to intensity change, *Mon. Weather Rev.*, *131*, 1783–1797.

Davis, A., and X.-H. Yan (2004), Hurricane forcing on chlorophyll-*a* concentration off the northeast coast of the U.S., *J. Geophys. Res.*, *31*, L17304, doi:10.1029/2004GL020668.

Foltz, G. R., K. Balaguru, and L. R. Leung (2015), A reassessment of the integrated impact of tropical cyclones on surface chlorophyll in the western subtropical North Atlantic, *Geophys. Res. Lett.*, *42*, 1158–1164, doi:10.1002/2015GL063222.

Gierach, M. M., and B. Subrahmanyam (2008), Biophysical responses of the upper ocean to major Gulf of Mexico hurricanes in 2005, *J. Geophys. Res.*, *113*, C04029, doi:10.1029/2007JC004419.

Hanshaw, M. N., M. S. Lozier, and J. B. Palter (2008), Integrated impact of tropical cyclones on sea surface chlorophyll in the North Atlantic, *Geophys. Res. Lett.*, *35*, L01601, doi:10.1029/2007GL031862.

Jacob, S. D., L. K. Shay, A. J. Mariano, and P. G. Black (2000), The 3D oceanic mixed layer response to Hurricane Gilbert, *J. Phys. Oceanogr.*, *30*, 1407–1429, doi:10.1175/1520-0485.

Kimball, S. K., and M. S. Mulekar (2004), A 15-year climatology of North Atlantic tropical cyclones. Part I: Size parameters, *J. Clim.*, *17*, 3555–3575, doi:10.1175/1520-0442.

Li, Y., and R. He (2014), Spatial and temporal variability of SST and ocean color in the Gulf of Maine based on cloud-free SST and chlorophyll reconstructions in 2003–2012, *Remote Sens. Environ.*, *144*, 98–108, doi:10.1016/j.rse.2014.01.019.

Lin, I., W. T. Liu, C.-C. Wu, G. T. F. Wong, C. Hu, Z. Chen, W.-D. Liang, Y. Yang, and K.-K. Liu (2003), New evidence for enhanced ocean primary production triggered by tropical cyclone, *Geophys. Res. Lett.*, *30*(13), 1718, doi:10.1029/2003GL017141.

Merritt-Takeuchi, A., and S. Chiao (2013), Case studies of tropical cyclones and phytoplankton blooms over Atlantic and Pacific Regions, *Earth Interact.*, *17*, 1–19, doi:10.1175/2013EI000517.1.

Miles, T. N., and R. He (2010), Temporal and spatial variability of chl-*a* and SST on the South Atlantic Bight: Revisiting with cloud-free reconstructions of MODIS satellite imagery, *Cont. Shelf Res.*, *30*, 1951–1962, doi:10.1016/j.csr.2010.08.016.

Miles, T. N., R. He, and M. Li (2009), Characterizing the South Atlantic Bight seasonal variability and cold-water event in 2003 using a daily cloud-free SST and chlorophyll analysis, *Geophys. Res. Lett.*, *36*, L02604, doi:10.1029/2008gl036396.

Paternoster, R., R. Brame, P. Mazerolle, and A. Piquero (1998), Using the correct statistical test for the equality of regression coefficients, *Criminology*, *36*, 859–866, doi:10.1111/j.1745-9125.1998.tb01268.x.

Price, J. F. (1981), Upper ocean response to a hurricane, *J. Phys. Oceanogr.*, *11*, 153–175, doi:10.1175/1520-0485.

Sanford, T. B., P. G. Black, J. R. Haustein, J. W. Feeney, G. Z. Forristall, and J. F. Price (1987), Ocean response to a hurricane. Part I: Observations, *J. Phys. Oceanogr.*, *17*, 2065–2083, doi:10.1175/1520-0485.

Shay, L. K., and R. L. Elsberry (1987), Near-inertial ocean current response to Hurricane Frederic, *J. Phys. Oceanogr.*, *17*, 1249–1269, doi:10.1175/1520-0485.

Walker, N. D., R. R. Leben, and S. Balasubramanian (2005), Hurricane-forced upwelling and chlorophyll *a* enhancement within cold-core cyclones in the Gulf of Mexico, *Geophys. Res. Lett.*, *32*, L18610, doi:10.1029/2005GL023716.

Wentz, F. K., C. Gentemann, D. Smith, and D. Chelton (2000), Satellite measurements of sea surface temperature through clouds, *Science*, *288*, 847–850.

Zhao, Y., and R. He (2012), Cloud-free sea surface temperature and colour reconstruction for the Gulf of Mexico: 2003–2009, *Remote Sens. Lett.*, *3*, 697–706, doi:10.1080/01431161.2012.666638.